

# The influence of potassium concentration on epileptic seizures in a coupled neuronal model in the hippocampus

Mengmeng Du<sup>1</sup> · Jiajia Li<sup>1</sup> · Rong Wang<sup>1</sup> · Ying Wu<sup>1</sup>

Received: 20 October 2015 / Revised: 14 March 2016 / Accepted: 19 May 2016 / Published online: 27 May 2016  
© Springer Science+Business Media Dordrecht 2016

**Abstract** Experiments on hippocampal slices have recorded that a novel pattern of epileptic seizures with alternating excitatory and inhibitory activities in the CA1 region can be induced by an elevated potassium ion ( $K^+$ ) concentration in the extracellular space between neurons and astrocytes (ECS-NA). To explore the intrinsic effects of the factors (such as glial  $K^+$  uptake,  $Na^+-K^+-ATPase$ , the  $K^+$  concentration of the bath solution, and  $K^+$  lateral diffusion) influencing  $K^+$  concentration in the ECS-NA on the epileptic seizures recorded in previous experiments, we present a coupled model composed of excitatory and inhibitory neurons and glia in the CA1 region. Bifurcation diagrams showing the glial  $K^+$  uptake strength with either the  $Na^+-K^+-ATPase$  pump strength or the bath solution  $K^+$  concentration are obtained for neural epileptic seizures. The  $K^+$  lateral diffusion leads to epileptic seizure in neurons only when the synaptic conductance values of the excitatory and inhibitory neurons are within an appropriate range. Finally, we propose an energy factor to measure the metabolic demand during neuron firing, and the results show that different energy demands for the normal discharges and the pathological epileptic seizures of the coupled neurons.

**Keywords** Epileptic seizures · Chemical synapse ·  $K^+$  lateral diffusion · Energy factor

## Introduction

Epilepsy, which seriously threatens the health of affected people, is one of the most common brain neurological disorders. As one of the most prevalent types of intractable epilepsy in clinics, temporal lobe epilepsy has a special clinical presentation with seizure-like activity (Prinz 2008).

Previous studies and experiments showed that elevated  $K^+$  concentration in the extracellular space between neurons and astrocytes (ECS-NA) could induce epileptic activity (Traynelis and Dingledine 1988; Marom et al. 2003; Bazhenov et al. 2004; Fröhlich et al. 2008). In particular, Ullah et al. found that excitatory neurons in the CA1 region of rat hippocampal slices could generate epileptic firing by increasing the ECS-NA  $K^+$  concentration and that excitatory neurons could enter a depolarization block phase when the peak of  $K^+$  concentration was approximately 40 mM (Ullah et al. 2009; Cressman et al. 2009). Many factors influence the  $K^+$  concentration in the ECS-NA:  $K^+$  currents across the neuronal membrane, glial uptake,  $Na^+/K^+-ATPase$  pumps, the spatial diffusion of  $K^+$  in the ECS-NA, and the  $K^+$  lateral diffusion between neurons and cotransporters (Kager et al. 2000, 2007; Larsen et al. 2014; Øyehaug et al. 2012; Yina et al. 2014b; Østby 2009; Durand and Jensen 2010). Which of these factors that influences the  $K^+$  concentration in the ECS-NA could induce epileptic seizures? A number of results from biological experiments have answered this question (Ohno et al. 2015; Cornog et al. 1967; Traynelis and Dingledine 1988; Durand and Jensen 2010; Park and Durand 2006). In 2015, Ohno found that down-regulation or dysfunction of  $K^+$  uptake channels (Kir4.1) in astrocytes could induce tonic-clonic seizures events and proposed that activation or up-regulation of  $K^+$  uptake channels (Kir4.1) would be a

✉ Ying Wu  
wyng36@163.com

<sup>1</sup> State Key Laboratory for Strength and Vibration of Mechanical Structures, School of Aerospace, Xi'an Jiaotong University, Xi'an, China

novel approach for the treatment of epilepsy (Ohno et al. 2015). Moreover, inhibition of  $\text{Na}^+/\text{K}^+$ -ATPase enzyme activity by ouabain could induce seizure discharges (Cornog et al. 1967). Furthermore, Traynelis found that excitatory neurons exhibited spontaneous periodic seizures in the CA1 region of rat hippocampal slices in the absence of external input when  $K_{\text{bath}}$  was increased to 8.5 mM (Traynelis and Dingledine 1988). Additionally, the studies of Durand and Park supported the view that the  $\text{K}^+$  lateral diffusion could lead to the generation of non-synaptic epilepsy in zero- $\text{Ca}^{2+}$  in excitatory neuronal networks in the CA1 area (Durand and Jensen 2010; Park and Durand 2006). Therefore, studying the relations between these factors that affect the  $\text{K}^+$  concentration in the ECS-NA and epileptic discharges through a theoretical analysis method would provide strong guidance for preventing and treating epilepsy.

At present, some studies have used a theoretical analysis method to explore the relationship between the  $\text{K}^+$  concentration in the ECS-NA and epileptic activities. In 2009, Cressman constructed a mathematical model consisting of a single conductance-based neuron and considered the intra- and extra-neuronal dynamic  $\text{K}^+$  concentrations; the researchers hypothesized that the  $\text{K}^+$  concentration in the ECS-NA was continuously adjusted by  $\text{K}^+$  currents across the neuronal membrane, glial uptake,  $\text{Na}^+/\text{K}^+$ -ATPase pumps and  $\text{K}^+$  spatial diffusion (Cressman et al. 2009). They described the bifurcation analysis of these factors affecting the  $\text{K}^+$  concentration in the ECS-NA. On the basis of the single neuron model proposed by Cressman and Yina added the dynamics of the intra- and extra-neuronal  $\text{Cl}^-$  concentrations and the oxygen dynamics, and she determined that the rate of change in the  $\text{K}^+$  concentration in the ECS-NA was not only a function of the factors proposed by Cressman but also a function of the glial  $\text{Na}^+/\text{K}^+$  pump current,  $\text{Na}^+/\text{K}^+/2\text{Cl}^-$  cotransporter current and  $\text{K}^+/\text{Cl}^-$  cotransporter current (Yina et al. 2014b). This study provided a two-parameter bifurcation diagram for the  $\text{K}^+$  concentration in the ECS-NA as a function of the bath oxygen concentration and the bath  $\text{K}^+$  concentration; the diagram showed the parameter regions that corresponded to the normal state and the different pathological discharge states of neurons. Furthermore, the brain includes a huge network of excitatory and inhibitory neurons whose interaction generate normal brain activities, and the interplay between excitatory and inhibitory neurons could generate epileptiform activity in *in vitro* experiments (Ziburkus et al. 2006; Žiburkus et al. 2013). Ullah presented a computational model composed of excitatory and inhibitory neurons in the CA1 region; these two types of neurons were coupled by both synaptic connections and  $\text{K}^+$  lateral diffusion. In this model, each neuron had its own extracellular microenvironment, such as  $\text{K}^+$  spatial diffusion

and glial uptake. This report incorporated the coupled model into a predictor-controller framework from modern control theory to reconstruct the extracellular microenvironment and activities of different types of neurons during seizures (Ullah and Schiff 2010). In 2014, Yina introduced oxygen dynamics to the coupled model of Ullah and provided the two-parameter bifurcation diagrams for the glial  $\text{K}^+$  uptake strength and the  $\text{K}^+$  spatial diffusion rate for the alternating interplay in epileptic discharge (Yina et al. 2014a). She also obtained the time series of oxygen consumption during epileptic firing in the coupled model. Regarding factors influencing  $\text{K}^+$  concentration in the ECS-NA and seizures, studies ignored the effect of the bath  $\text{K}^+$  concentration,  $\text{Na}^+/\text{K}^+$ -ATP pumps, and the  $\text{K}^+$  lateral diffusion between neurons on seizures and the prominent role of glial  $\text{K}^+$  uptake in the generation of epileptic activities in a coupled model.

Synaptic connections are the primary type of connection in biological systems. The lack of balance between excitatory and inhibitory synaptic conductance controls the hyper-excitability and recurrent seizures in neuronal networks (Žiburkus et al. 2013). The studies of Durand (Durand and Jensen 2010) and Park ignored the synaptic connections between neurons in their research on the relationship between  $\text{K}^+$  lateral diffusion coupling and the generation of non-synaptic epilepsy in excitatory neuronal networks. Therefore, in the calculation model of excitatory and inhibitory neurons coupled by both synaptic connections and  $\text{K}^+$  lateral diffusion, an interesting question remains: Is there a dependency between  $\text{K}^+$  lateral diffusion and synaptic conductance in the generation of seizures?

Another important issue relates to the energy expenditure for neuronal network activity. The generation of an action potential in neurons is an energy-consuming process, and metabolic energy is required to maintain the normal signaling activity of neurons. Pathological brain activities would take place if the energy supply is not sufficient to satisfy the metabolic consumption, such as during seizures (Bahar et al. 2006; Ingram et al. 2013). Hence, the energy consumption during the normal and epileptic discharge of coupled excitatory and inhibitory neurons should be considered.

In this paper, which is based on the coupled model described by Ullah and Schiff (2010) and Yina et al. (2014a), we further evaluated the neuronal firing pattern with various bath  $\text{K}^+$  concentrations in “Elevated bath  $\text{K}^+$  concentration can induce epileptic seizures” section. Moreover, we analyzed how the bath  $\text{K}^+$  concentration is related to the glial  $\text{K}^+$  uptake and  $\text{Na}^+/\text{K}^+$ -ATP pumps during epileptic seizures in “The role of glial  $\text{K}^+$  uptake in the development of epileptic seizures” section. Furthermore, the dependency of  $\text{K}^+$  lateral diffusion

and synaptic conductance between two neurons in the generation of epileptic activity is discussed in “The influences of  $K^+$  lateral diffusion and synaptic coupling on epileptic seizures” section. Finally, we introduced an energy factor to explore energy consumption during normal firing and epileptic seizures in “The energy consumption in epileptic seizures” section.

### Model and method

In this section, using the coupled model in Ullah and Schiff (2010) and Yina et al. (2014a) studies, we present a similar coupled model composed of excitatory and inhibitory neurons with synaptic connections and  $K^+$  lateral diffusion. In this model, an excitatory neuron innervates inhibitory neurons via excitatory synapses (AMPA) (Graham et al. 2012), whereas an inhibitory neuron innervates excitatory neurons via inhibitory synapses (GABAA) (Wendling et al. 2012). The sketch is shown in Fig. 1.

We assume that excitatory and inhibitory neurons have different local architectures. The excitatory neuron model has  $I_{Na}$ ,  $I_K$ , leak current  $I_L$  (Ullah et al. 2009), after-hyperpolarization current  $I_{AHP}$ , and inhibitory postsynaptic current  $I_{syn,GABA}$  and external stimulation current  $I_{ext}$ . The inhibitory neuron model includes  $I_{Na}$ ,  $I_K$ , leak current  $I_L$  (Ullah et al. 2009), and excitatory postsynaptic currents  $I_{syn,AMPA}$  and external stimulation current  $I_{ext}$ .

The H–H-type dynamic equations for the two neurons are as follows:

$$C \frac{dV_{En}}{dt} = -I_{Na} - I_K - I_L - I_{AHP} + I_{syn,GABA} + I_{ext} \quad (1)$$

$$C \frac{dV_{In}}{dt} = -I_{Na} - I_K - I_L + I_{syn,AMPA} + I_{ext} \quad (2)$$

where  $C$  is the membrane capacitance. The voltage-gated currents  $I_{Na}$  and  $I_K$ , the leak current  $I_L$ , and the after-hyperpolarization current  $I_{AHP}$  in Eqs. (1) and (2) are:

$$\begin{aligned} I_{Na} &= -g_{Na}m^3h(V - V_{Na}) \\ I_K &= -g_Kn^4(V - V_K) \\ I_{AHP} &= -\left(\frac{g_{AHP}[Ca]_i}{1 + [Ca]_i}\right)(V - V_K) \\ I_L &= -g_{NaL}(V - V_{Na}) - g_{KL}(V - V_K) - g_{Cl}(V - V_{Cl}) \end{aligned} \quad (3)$$

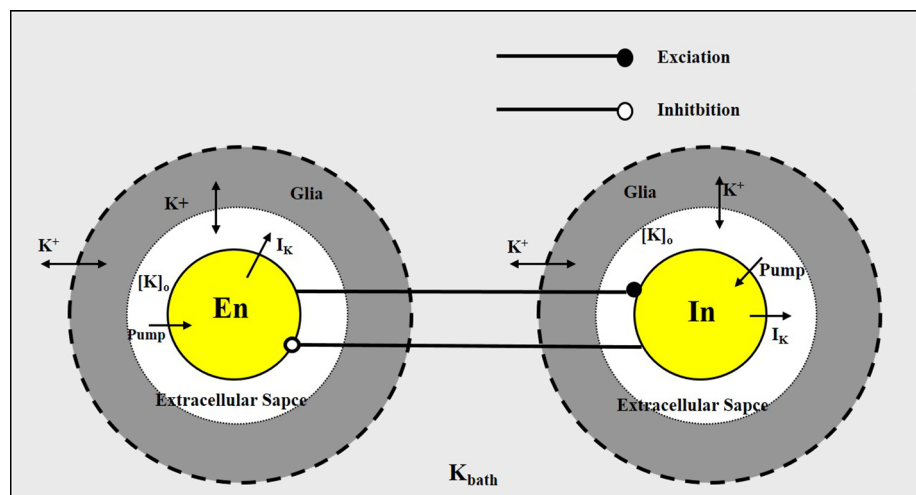
where  $g_{Na}$  and  $g_K$  denote the conductances corresponding to the sodium and potassium currents, respectively.  $g_{AHP}$  is the conductance corresponding to the after-hyperpolarization current.  $g_{NaL}$  and  $g_{KL}$  are the conductances corresponding to the sodium leak current and potassium leak current, respectively.  $V_{Na}$ ,  $V_K$  and  $V_{Cl}$  denote the  $Na^+$ ,  $K^+$  and  $Cl^-$  channel reversal potentials, respectively.  $n$ ,  $m$  and  $h$  are gating variables for sodium and potassium currents.  $g_{Ca}$  and  $V_{Ca}$  are the conductance and the reversal potential of calcium respectively.  $[Ca]_i$  corresponds to the intracellular calcium concentration, and the dynamics equation is:

$$\begin{aligned} \frac{d[Ca]_i}{dt} &= -0.002g_{Ca}(V - V_{Ca})/\{1 + \exp(-(V + 25)/2.5)\} \\ &\quad - [Ca]_i/80 \end{aligned} \quad (4)$$

The equations for the gating variables in Eq. (3) are:

$$\frac{dq}{dt} = \varphi[\alpha_q(V)(1 - q) - \beta_q(V)q], \quad q = m, n, h \quad (5)$$

**Fig. 1** Model reproducing the hippocampal CA1 area activity



$$\begin{aligned}\alpha_m &= 0.1(V + 30)/[1 - \exp(-0.1(V + 30))] \\ \beta_m &= 4 \exp[-(V + 55)/18] \\ \alpha_n &= 0.01(V + 34)/[1 - \exp(-0.1(V + 34))] \\ \beta_n &= 0.125 \exp(-(V + 44)/80) \\ \alpha_h &= 0.07 \exp(-(V + 44)/20) \\ \beta_h &= 1/[1 + \exp(-0.1(V + 14))]\end{aligned}$$

The reversal potential of the  $\text{Cl}^-$  current is equal to a fixed value ( $V_{\text{Cl}} = -81.93$  mV). The reversal potentials of  $\text{Na}^+$  and  $\text{K}^+$  are given by the Nernst equation:

$$\begin{aligned}V_{\text{Na}} &= 26.64 \ln\left(\frac{[\text{Na}]_o}{[\text{Na}]_i}\right) \\ V_{\text{K}} &= 26.64 \ln\left(\frac{[\text{K}]_o}{[\text{K}]_i}\right)\end{aligned}\quad (6)$$

where  $[\text{Na}]_i$  and  $[\text{Na}]_o$  denote the sodium ion concentrations in the intra-neuronal and extra-neuronal spaces, respectively, and  $[\text{K}]_i$  and  $[\text{K}]_o$  denote the potassium ion concentration in the intra-neuronal and extra-neuronal spaces, respectively. The  $[\text{K}]_o$  value is continuously updated by the  $\text{K}^+$  currents across the neuronal membrane,  $\text{Na}^+/\text{K}^+$ -ATP pumps, glial uptake,  $\text{K}^+$  spatial diffusion (Cressman et al. 2008; Ullah and Schiff 2010), and  $\text{K}^+$  lateral diffusion between neurons. Thus, the  $\text{K}^+$  concentration dynamics in the extraneuronal space is modeled as follows:

$$\begin{aligned}\frac{d[\text{K}]_o}{dt} &= -0.33I_{\text{K}} - 2\beta I_{\text{pump}} - I_{\text{glia}} - I_{\text{diff}} - I_{\text{lateral},ij} \quad (7) \\ I_{\text{pump}} &= \rho \left( \frac{1}{1.0 + \exp(25.0 - [\text{Na}]_i/3.0)} \right) \times \left( \frac{1}{1 + \exp(8 - [\text{K}]_o)} \right) \\ I_{\text{glia}} &= G \left( \frac{1}{1.0 + \exp((18.0 - [\text{K}]_o)/2.5)} \right) \\ I_{\text{diff}} &= \varepsilon([\text{K}]_o - k_{\text{bath}})\end{aligned}$$

The dimensionless factor  $\beta$  accounts for the ratio of the intracellular volume to the extracellular volume for calculations of the concentration change,  $\rho$  is the pump strength of  $\text{Na}^+/\text{K}^+$ -ATP,  $[\text{Na}]_i$  is the intracellular sodium concentration,  $G$  is the glial uptake strength for  $\text{K}^+$ ,  $\varepsilon$  is the spatial diffusion coefficient of  $\text{K}^+$ , and  $k_{\text{bath}}$  is the  $\text{K}^+$  concentration in the largest nearby reservoir.

The  $\text{K}^+$  concentration dynamics in the intra-neuronal space is

$$[\text{K}]_i = 140 \text{ mM} + (18.0 \text{ mM} - [\text{Na}]_i) \quad (8)$$

The intra- and extra-cellular  $\text{Na}^+$  concentration dynamics are modeled as follows (Cressman et al. 2008; Ullah and Schiff 2010):

$$\begin{aligned}\frac{d[\text{Na}]_i}{dt} &= 0.33 \frac{I_{\text{Na}}}{\beta} - 3I_{\text{pump}} \\ [\text{Na}]_o &= 144 \text{ mM} - \beta([\text{Na}]_i - 18.0 \text{ mM})\end{aligned}\quad (9)$$

In Eq. (8),  $I_{\text{pump}}$  in Eqs. (7) and (9) is multiplied by factors of 2 and 3, respectively, because the  $\text{K}^+$ - $\text{Na}^+$  pump has an electrogenic ratio of 2:3 (Cressman et al. 2008; Ullah and Schiff 2010).

The  $\text{K}^+$  lateral diffusion current between two neurons is described as follows:

$$I_{\text{lateral},ij} = \frac{D_{\text{K}}}{\Delta x_{ij}^2} ([\text{K}]_o^j - [\text{K}]_o^i) \quad (10)$$

where  $i$  and  $j$  represent excitatory and inhibitory neurons, respectively.  $\Delta x_{ij}$  is the distance between two neurons, and  $D_{\text{K}}$  is the diffusion factor of  $\text{K}^+$ .

The inhibitory synaptic current  $I_{\text{syn},\text{GABA}}$  in the membrane potential equation [Eq. (1)] can be described as (Pinsky et al. 1994; Ermentrout and Terman 2010):

$$\begin{aligned}I_{\text{syn},\text{GABA}} &= g_{\text{GABA}} S_{\text{GABA}} (V_{\text{En}} - V_{\text{GABA}}) \quad (11) \\ \frac{dS_{\text{GABA}}}{dt} &= \alpha_{\text{GABA}} F(V_{\text{GABA}})(1 - S_{\text{GABA}}) - \beta_{\text{GABA}} S_{\text{GABA}} \\ F(V_{\text{GABA}}) &= \frac{1}{1 + \exp(-(V_{\text{In}} - 2.0)/5.0)}\end{aligned}$$

where  $g_{\text{GABA}}$  and  $V_{\text{GABA}}$  are the maximum conductance and the reversal potential, respectively, and  $S_{\text{GABA}}$  reflects the fraction of open receptor-operated ion channels.

The excitatory synaptic currents  $I_{\text{syn},\text{AMPA}}$  in the membrane potential equation [Eq. (2)] can be described as (Pinsky et al. 1994; Ermentrout and Terman 2010):

$$\begin{aligned}I_{\text{syn},\text{AMPA}} &= g_{\text{AMPA}} S_{\text{AMPA}} (V_{\text{In}} - V_{\text{AMPA}}) \quad (12) \\ \frac{dS_{\text{AMPA}}}{dt} &= \alpha_{\text{AMPA}} \frac{1}{1 + \exp(-(V_{\text{En}} - 2.0)/5.0)} (1 - S_{\text{AMPA}}) \\ &\quad - \beta_{\text{AMPA}} S_{\text{AMPA}}\end{aligned}$$

where  $g_{\text{AMPA}}$  is the maximum conductance, and  $S_{\text{AMPA}}$  describes the kinetics of the AMPA receptor.

The values of the parameters used in the model are listed in Table 1.

Here, we introduce an energy factor to describe the energy consumption during normal and pathological neuronal discharges. The total electrical energy accumulated in the H–H model at a given moment is (Moujahid et al. 2012):

$$P(t) = \frac{1}{2} CV^2 + H_{\text{Na}} + H_{\text{K}} + H_{\text{Cl}} \quad (13)$$

The total derivative with respect to time of the above energy will be:

**Table 1** Model parameters

Parameter	Value and units	Description
$C$	1 $\mu\text{F}/\text{cm}^2$	Membrane capacitance
$g_{\text{Na}}$	100 $\text{mS}/\text{m}^2$	Conductance of the persistent sodium current
$g_{\text{K}}$	40 $\text{mS}/\text{m}^2$	Conductance of the potassium current
$g_{\text{AHP}}$	0.01 $\text{mS}/\text{m}^2$	Conductance of the after-hyperpolarization current
$g_{\text{KL}}$	0.05 $\text{mS}/\text{m}^2$	Conductance of the potassium leak current
$g_{\text{NaL}}$	0.05 $\text{mS}/\text{m}^2$	Conductance of the sodium leak current
$g_{\text{Cl}}$	0.05 $\text{mS}/\text{m}^2$	Conductance of the chloride leak current
$g_{\text{Ca}}$	0.1 $\text{mS}/\text{m}^2$	Calcium conductance
$V_{\text{Ca}}$	120 mV	Reversal potential for the chloride current
$\beta$	7.0	Reversal potential for calcium
$\rho$	1.25 mM/s	Pump strength of the neuron
$G$	66 mM/s	Strength of glial uptake
$\varepsilon$	1.2 $\text{s}^{-1}$	Diffusion constant
$K_{\text{Kbath}}$	4.0 mM	Steady-state extracellular potassium concentration
$[Cl]_i$	6.0 mM	Intracellular chloride concentration
$[Cl]_o$	130.0 mM	Extracellular chloride concentration
$\alpha_{\text{GABA}}$	0.18 $\text{ms}^{-1}$	The rise rate of the GABAA synaptic conductance
$\beta_{\text{GABAA}}$	5.0 $\text{mM}^{-1}/\text{ms}$	The decay rate of the GABAA synaptic conductance
$\alpha_{\text{AMPA}}$	1.1 $\text{mM}^{-1}/\text{ms}$	The rise rate of the AMPA synaptic conductance
$\beta_{\text{AMPA}}$	0.19 $\text{ms}^{-1}$	The decay rate of the AMPA synaptic conductance

$$\dot{P} = VI - I_{\text{Na}}(V - E_{\text{Na}}) - I_{\text{K}}(V - E_{\text{K}}) - I_{\text{Cl}}(V - E_{\text{Cl}}) \quad (14)$$

where the current  $I$  denotes the sum of the external stimulus current and the synaptic current in Eqs. (1) and (2).

Here, we obtain the energy factor during neuron firing (Moujahid et al. 2012).

$$P = \int_0^T \left( VI - g_{\text{Na}} m^3 h (V - E_{\text{Na}})^2 - g_{\text{K}} n^4 (V - E_{\text{K}})^2 - g_{\text{Cl}} (V - E_{\text{Cl}})^2 \right) dt \quad (15)$$

For numerical simulations, we assume that excitatory and inhibitory neurons share the same bath potassium concentration [that is, excitatory and inhibitory neurons have the same value of  $K_{\text{bath}}$  in Eq. (7)]. The 4th-order Runge–Kutta method is used for the numerical simulation with a time step  $h = 0.01$  ms. Meanwhile, parameter values in numerical simulation are shown in Table 1 if there is no special emphasis.

### Elevated bath $\text{K}^+$ concentration can induce epileptic seizures

In this section, to test some of the experimental results published in other studies (Jensen and Yaari 1997; Traynelis and Dingledine 1988; Gluckman et al. 2001; Ziburkus et al. 2006; Ziburkus et al. 2013) showing that for slice

preparations in the absence of an external stimulus input, neural networks are usually in different firing states when the value of the bath potassium concentration ( $K_{\text{bath}}$ ) [which is mentioned in Eq. (7)] varies, thus, Fig. 2 shows firing patterns of the coupled inhibitory and excitatory neurons under different values of  $K_{\text{bath}}$ . Both neurons maintain a normal resting potential when  $K_{\text{bath}}$  is 4 mM, as shown in Fig. 2a. However, an alternating and periodic seizure firing event occurs when  $K_{\text{bath}}$  is 8.5 mM, as shown in Fig. 2b. During this epileptic firing process, when the excitatory neuron is silent, the inhibitory neuron is intensively firing, and following intense firing, the inhibitory neuron enters a state of depolarization block. Simultaneously, the excitatory neuron shows intense epileptiform firing. This periodic epileptic firing is consistent with the experimental phenomenon observed in slices of the hippocampal CA1 region (Traynelis and Dingledine 1988; Ziburkus et al. 2006; Ziburkus et al. 2013). Furthermore, as  $K_{\text{bath}}$  is increased to 24 mM, the neurons show another type of periodic seizure: both neurons simultaneously and periodically enter a phase of depolarization block, as shown in Fig. 2c. Through the analysis of discharge modes for various values of  $K_{\text{bath}}^+$ , we can better test the experimental observations (Ziburkus et al. 2006; Ziburkus et al. 2013; Traynelis and Dingledine 1988) indicating that an elevated potassium bath concentration ( $K_{\text{bath}}$ ) can induce periodic seizures in the coupled excitatory and inhibitory neuronal model.

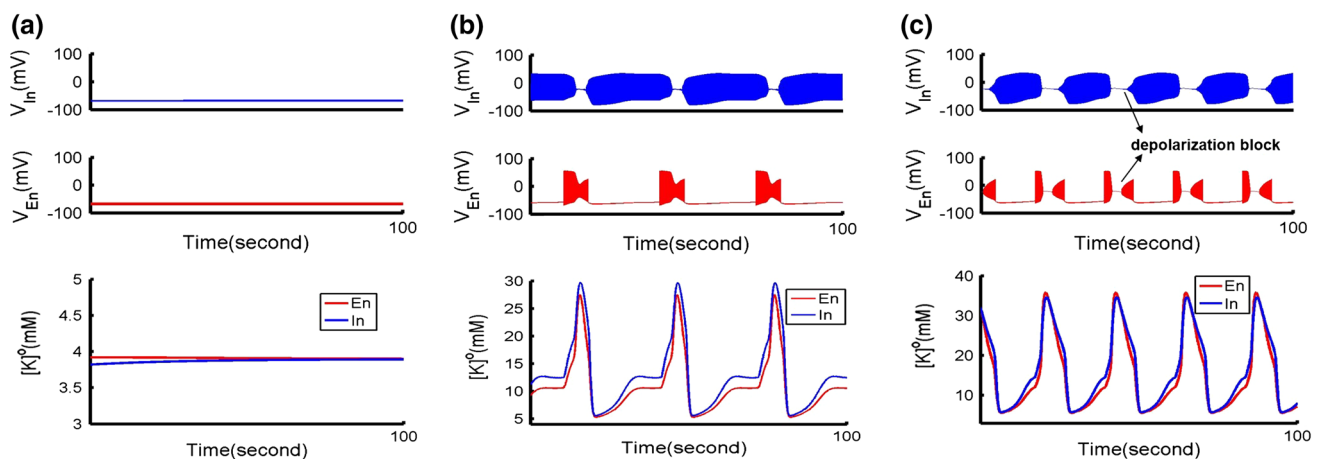


**Fig. 2** Elevated  $K_{bath}$  can induce epileptic seizures in the coupled excitatory and inhibitory neuronal model. **a** Resting states of neurons when  $K_{bath}$  is 4 mM, **b** periodic spontaneous seizures when  $K_{bath}$  is

8.5 mM. **c** The two neurons periodically enter a phase of depolarization block simultaneously when  $K_{bath}$  is 24 mM

Meanwhile, in the time series of the  $K^+$  concentration oscillation in the ECS-NA, which corresponds to two types of epileptic seizures in Fig. 2b, c, we can see that the peak of  $K^+$  concentration in the ECS-NA ( $[K^+]_o$ ) is approximately 29 mM when the inhibitory neuron enters the phase of depolarization block with  $K_{bath} = 8.5$  mM; however, the peak of  $K^+$  concentration in the ECS-NA ( $[K^+]_o$ ) is close to 40 mM when the depolarization block stage occurs simultaneously for both neurons at  $K_{bath} = 24.0$  mM. This result shows that different epileptic activities are accompanied by different high-amplitude oscillations of the  $K^+$  concentration in the ECS-NA.

### The role of glial $K^+$ uptake in the development of epileptic seizures

Here, to examine the threshold of  $Na^+-K^+$ -ATPase pump strength ( $\rho$ ), glial  $K^+$  uptake strength ( $G$ ), and bath  $K^+$  concentration ( $K_{bath}$ ) for the pathological epileptic activities of neurons, we plot the bifurcation diagrams shown in Fig. 3. First, a two-parameter bifurcation diagram of  $G$  and  $\rho$  provides a more complete understanding of the epileptic discharges in the coupled model with respect to the variation of both  $G$  and  $\rho$  of the excitatory neuron, with  $k_{bath} = 8.0$  mM, as shown in Fig. 3a. The blue parameter area shows that  $G$  is sufficiently large for a normal firing state of the neurons, and the green area shows a parameter space that supports alternating epileptic firing, which was reported for an experimental recording (Ziburkus et al. 2006; Žiburkus et al. 2013). It means that if  $G$  is reduced from the blue parameter area to green region, epileptic events occur in the neurons, this is because the removing function of glia is impaired when it is working at making

$K^+$  away from the ECS-NA. The yellow region indicates another type of periodic seizure in which the two neurons simultaneously and periodically enter a phase of depolarization block and the red area indicates a pathological limit state in which the excitatory neuron presents persistent high-frequency firing and inhibitory neuron is in a state of slight oscillation near 20 mV. Further, Fig. 3b shows a double-parameter space of  $G$  and  $K_{bath}$  for different firing pattern of neurons; the values of  $G$  and  $K_{bath}$  for the excitatory neuron are varied. The discharge patterns of the neurons for each color of the parameter region are consistent with Fig. 3a. From the two double-parameter bifurcation diagrams, we find that only increasing the glial  $K^+$  uptake strength ( $G$ ) can terminate pathological seizures. However, in contrast to the effects of the glial  $K^+$  uptake strength ( $G$ ), the state of pathological discharge can not be terminated by changing  $Na^+-K^+$ -ATPase pump ( $\rho$ ) or bath  $K^+$  concentration ( $K_{bath}$ ) when the glial  $K^+$  uptake strength ( $G$ ) is below its normal values. This result highlights the important role of glial  $K^+$  uptake in maintaining normal firing.

To further understand the role of the glial  $K^+$  uptake strength ( $G$ ) in neural firing patterns in the coupled model, we decrease  $G$  gradually and fix  $K_{bath} = 18.2$  mM, that is, changing  $G$  along the vertical dashed line in Fig. 3b. Figure 4 shows the membrane voltage of the inhibitory neuron (upper traces) and the excitatory neuron (lower traces) corresponding to the points 1, 2, 3, 4 in Fig. 3b. At point 1 in Fig. 3a ( $G = 39.7$  mM/s and  $K_{bath} = 18.2$  mM), the excitatory neuron is in a low-frequency bursting state, and the inhibitory neuron can generate persistent spike firing, as shown in Fig. 4a. Here, the glial  $K^+$  uptake is sufficiently strong such that neurons can maintain a normal discharge state beyond its epileptic firing

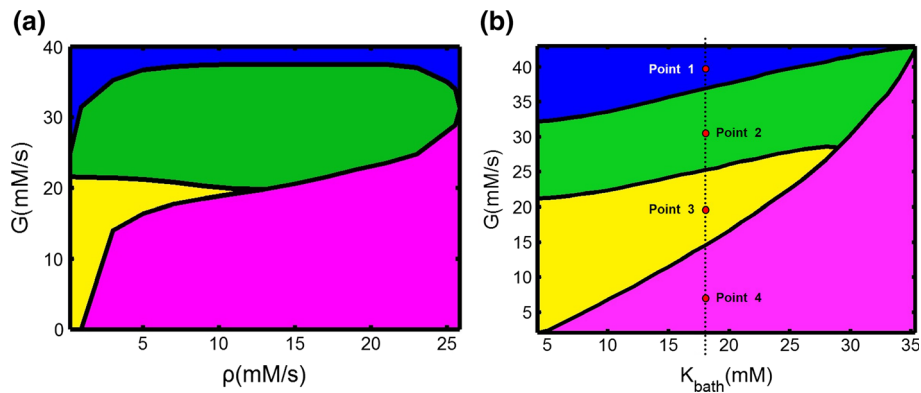
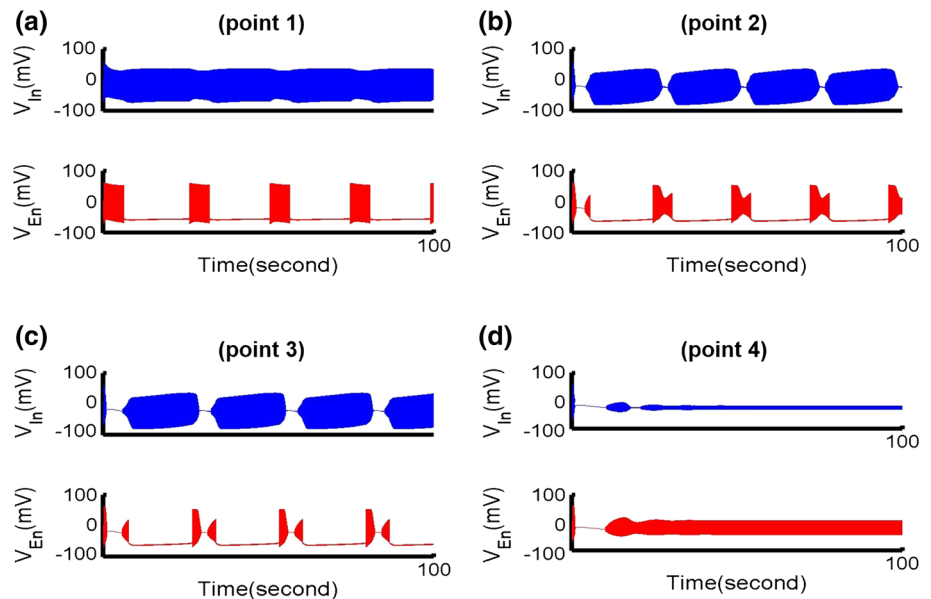


**Fig. 3** Two-parameter space diagrams for the glial K<sup>+</sup> uptake strength ( $G$ ) as a function of **a** the Na<sup>+</sup>-K<sup>+</sup>-ATPase pump strength ( $\rho$ ) and **b** the bath K<sup>+</sup> concentration  $K_{bath}$ . In both **a** and **b**, the blue area represents a state of normal firing. The green area shows a parameter space that supports alternating epileptic firing, as in an experimental recording (Ziburkus et al. 2006; Ziburkus et al. 2013).

The yellow parameter region indicates another type of periodic seizure in which both neurons will simultaneously and periodically enter a phase of depolarization block. The red area indicates a pathological limit state in which the excitatory neuron exhibits persistent firing and the inhibitory neuron is in a state of slight oscillation near 20 mV. (Color figure online)

**Fig. 4** Examples of the dynamics of the coupled inhibitory and excitatory neuron model obtained at parameter values corresponding to the numbered points (point 1–4) along the vertical dash line in Fig. 3b; the top trace and the bottom trace show the membrane voltages of inhibitory and excitatory neurons, respectively, on the same time scale



threshold. However, decreasing  $G$  to point 2 ( $G = 30.8$  mM/s) in Fig. 3b, the excitatory and inhibitory neurons transition from normal discharges to the typical alternating seizures reported in (Ziburkus et al. 2006; Ziburkus et al. 2013) during this firing pattern, inhibitory neurons are more active while excitatory neurons are in a silent state; this condition is followed by a period of depolarization block when the excitatory neuron exhibited runaway excitation, as shown in Fig. 4b. We also find that both inhibitory and excitatory neurons can periodically enter an epileptic state of depolarization block simultaneously (Fig. 4c) instead of alternating seizures at point 3 when  $G$  decreases to 19.6 mM/s. As  $G$  is further

decreased to  $G = 7.3$  mM/s (point 4 in Fig. 3b), the excitatory neuron can generate persistent firing, but the inhibitory neuron enters a state of slight oscillation near 20 mV, shown in Fig. 4d. This evolutionary model of neural firing patterns with  $G$  decreasing is caused by elevated K<sup>+</sup> concentration in the ECS-NA can induce epileptic firing of neurons. Besides, in this evolution pattern, the transition from pathological activities normal to discharge state of neurons suggests that seizure activity termination is characterized by the inhibitory neurons emerging from a depolarization block state into progressively more active spiking and the simultaneous gradual reduction of excitatory neuron spiking.

## The influences of $K^+$ lateral diffusion and synaptic coupling on epileptic seizures

The  $K^+$  lateral diffusion between neurons also influences the  $K^+$  concentration in the ECS-NA. Previous studies have found that the  $K^+$  lateral diffusion between two neurons is a significant factor for non-synaptic epileptogenesis in a low-calcium in vitro model (Yaari et al. 1986; Park and Durand 2006; Durand and Jensen 2010). Chemical synapses are abundant in the central nervous system. To clarify the role of  $K^+$  lateral diffusion and chemical synapse coupling in the generation of high  $K^+$ -induced epileptic activity, we present a two-parameter space for the conductance of inhibitory and excitatory synapses, in which epileptic firing can be induced only by  $K^+$  lateral diffusion, as seen in Fig. 5a. This result indicates that  $K^+$  lateral diffusion is a driving factor for the generation of pathological seizures only when the synaptic conductance of neural network is in an appropriate range. Moreover, Fig. 5b presents the curves for the threshold of  $D_K$  that will induce epileptic discharges as the conductance of the excitatory synapse increases for the following values of the inhibitory synapse: 0.12, 0.14 and 0.16 mS/cm<sup>2</sup>. The threshold of  $K^+$  lateral diffusion intensity ( $D_K$ ) that can induce epileptic discharges decreases as the excitatory synapse conductance increases gradually.

### The energy consumption in epileptic seizures

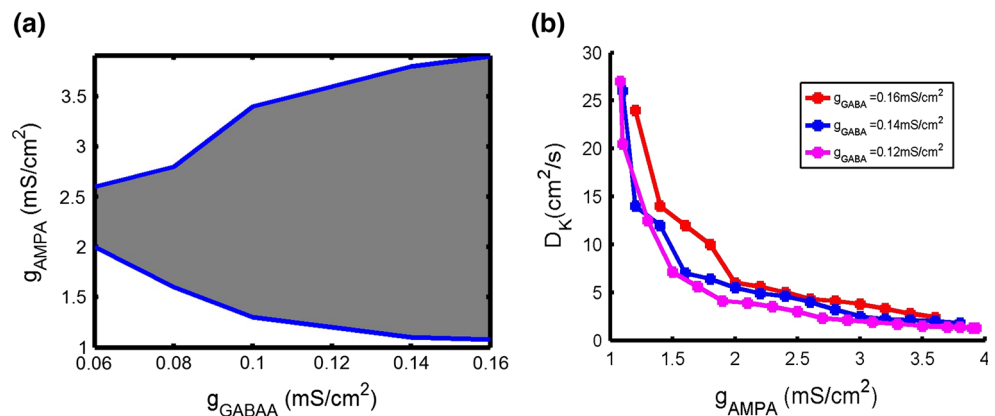
A mass of ions flowing across neural membranes is generated when various voltage-gated channels are activated during seizures, thus, increasing the metabolic energy demand. To estimate the energy consumption of the coupled neurons in different discharge patterns, an energy factor ( $P_i$ ,  $i = En$  or  $In$ ; thus,  $P_{En}$  and  $P_{In}$  denote the energy consumption values of excitatory and inhibitory neurons, respectively) is computed based on the H–H neuron model. Figure 6 presents the energy expenditure values of the

coupled excitatory and inhibitory neurons corresponding to different neuronal firing patterns as  $G$  decreases. In this figure, the points in solid boxes indicate the energy expenditure of neurons in a normal firing state, and the points in dashed boxes represent the energy expenditure of neurons in a pathological seizures state. The excitatory neuron consumes more energy during epileptic seizures than during the normal firing state. Accordingly, the corresponding coupled inhibitory neuron will consume less energy during an epileptic discharge process than in a normal firing state. To further distinguish the energy consumption in the seizure state, we calculate the energy consumption of neurons corresponding to different seizure firing patterns; for instance, point 2 in Fig. 6a, b corresponds to the energy consumption values of the alternating seizure firing pattern, and point 3 corresponds to the other type of seizure in which both neurons simultaneously enter a phase of depolarization block. The energy consumption of the excitatory neuron in the alternating seizure firing state (Fig. 4b) is smaller than the demand during the other type of seizure in which both neurons simultaneously enter a phase of depolarization block (Fig. 4c). This result shows the greater energy demand in the depolarization block process.

### Conclusion and discussion

In this paper, using a coupled model composed of excitatory and inhibitory neurons as well as glia in the CA1 region, we explored the intrinsic effect of the  $K^+$  concentration in the ECS-NA on the epileptic seizures observed in published experiments. First, we verified the experimental results showing that epileptic seizures can be induced directly in coupled excitatory and inhibitory neurons with no stimulus input when the bath  $K^+$  concentration is increased to a certain level. Meanwhile, different epileptic firing patterns are accompanied by different high-

**Fig. 5** **a** A two-parameter space as a function of  $g_{AMPA}$  and  $g_{GABAA}$  showing the boundary of the region in which epileptic firing can be induced by  $K^+$  lateral diffusion. **b** Curves showing the threshold of  $D_K$  that can induce epileptic firing in the coupled neural model when  $g_{AMPA}$  is increased for the following values:  $g_{GABAA} = 0.12, 0.14, 0.16$  mS/cm<sup>2</sup>





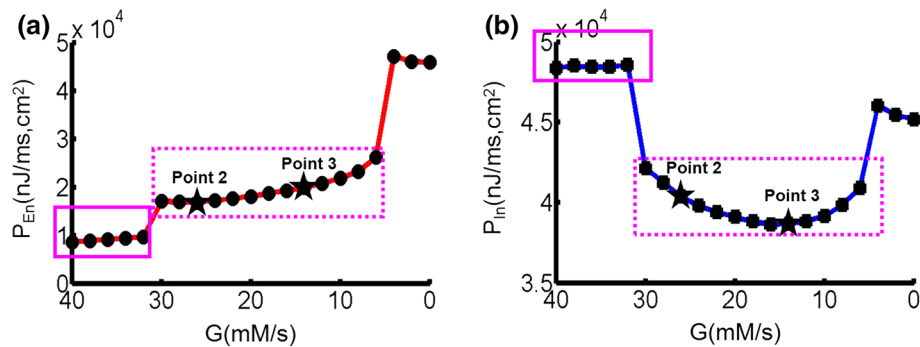


**Fig. 6** Metabolic energy consumption of an excitatory neuron (a) and an inhibitory neuron (b) corresponding to different neuronal firing patterns with  $G$  varying. The points in the *solid boxes* indicate the energy expenditure of excitatory and inhibitory neurons, respectively, that are in a normal firing state; the points in the *dashed boxes* indicate the energy expenditure of excitatory and inhibitory neurons, respectively, that are in a pathological seizures state

amplitude oscillations of the  $K^+$  concentration in the ECS-NA. For instance, as the peak of the  $K^+$  oscillation is 36.8 mM (which is close to 40 mM), inhibitory and excitatory neurons simultaneously enter a state of depolarization block.

Moreover, we presented the bifurcation parameter space of the glial  $K^+$  uptake strength ( $G$ ) with either the  $Na^+$ - $K^+$ -ATPase pump strength ( $\rho$ ) or the bath solution  $K^+$  concentration ( $K_{bath}$ ) during neural epileptic seizures occur. These diagrams highlighted the important role of glial  $K^+$  uptake in maintaining normal firing. We also described an evolutionary model of neural firing patterns with the strength of glial  $K^+$  uptake decreases; this model suggested that seizure activity termination is characterized by the inhibitory neurons emerging from a depolarization block state into a state of progressively more active spiking and the simultaneous gradual reduction of excitatory neuron spiking.

Furthermore, we observed that  $K^+$ -induced epileptic activity could be induced by  $K^+$  lateral diffusion between neurons only when the excitatory and inhibitory conductances are within an appropriate range. Additionally, as the excitatory synapse conductance value increases, less  $K^+$  lateral diffusion is needed to induce epileptic firing.

Finally, by analyzing the energy factor, we found that pathological seizures consume greater energy than normal discharge in excitatory neurons, especially for the depolarization block process during seizures. However, the energy consumption when inhibitory neurons entered the seizure process was smaller than for the normal firing state.

This paper aimed to provide an in-depth understanding of the factors influencing the  $K^+$  concentration in the ECS-NA and the energy consumption during epileptic seizures to facilitate the construction of more accurate dynamical models of neural networks to improve the recognition, forecasting and control of seizures.

respectively, that are in a normal firing state; the points in the *dashed boxes* indicate the energy expenditure of excitatory and inhibitory neurons, respectively, that are in a pathological seizures state

**Acknowledgments** This work is supported by National Natural Science Foundation of China under Grant Nos. 11272242 and 11472202 and Natural Science Foundation of Shaanxi Province of China (No. S2014JC12575).

## References

- Bahar S, Suh M, Zhao M et al (2006) Intrinsic optical signal imaging of neocortical seizures: the ‘epileptic dip’. *NeuroReport* 17(5):499–503
- Bazhenov M et al (2004) Potassium model for slow (2–3 Hz) in vivo neocortical paroxysmal oscillations. *J Neurophysiol* 92(2):1116–1132
- Cornog JL, Gonatas NK, Feierman JR (1967) Effects of intracerebral injection of ouabain on the fine structure of rat cerebral cortex. *Am J Pathol* 51(4):573–590
- Cressman JR, Ullah G, Ziburkus J et al (2009) The influence of sodium and potassium dynamics on excitability, seizures, and the stability of persistent states: I. Single neuron dynamics. *J Comput Neurosci* 26(2):159–170
- Durand DM, Jensen AL (2010) Potassium diffusive coupling in neural networks. *Philos Trans R Soc Lond* 365(1551):2347–2362
- Ermentrout BG, Terman D (2010) *Foundations of mathematical neuroscience*. Springer, New York, pp 157–167
- Fröhlich F, Timofeev I, Sejnowski TJ, Bazhenov M (2008) 26—Extracellular potassium dynamics and epileptogenesis. In: Soltesz I, Staley K (eds) *Computational Neuroscience in Epilepsy*, Academic press, New York, pp 419–439
- Gluckman BJ, Nguyen H, Schiff SJ (2001) Adaptive electric field control of epileptic seizures. *J Neurosci* 21(2): 590–600
- Graham BP, Saudargiene A, Cobb S (2012) A computational study of the influence of synaptic cooperativity on synaptic plasticity in a hippocampal CA1 pyramidal cell. *BMC Neurosci* 13(Suppl 1):P164
- Ingram JM, Zhang C, Xu J et al (2013) FRET excited ratiometric oxygen sensing in living tissue. *J Neurosci Methods* 214(1): 45–51
- Jensen MS, Yaari Y (1997) Role of intrinsic burst firing, potassium accumulation, and electrical coupling in the elevated potassium model of hippocampal epilepsy. *J Neurophysiol* 77(3):1224–1233
- Kager H, Wadman WJ, Somjen GG (2000) Simulated seizures and spreading depression in a neuron model incorporating interstitial space and ion concentrations. *J Neurophysiol* 84(1):495–512

- Kager H, Wadman WJ, Somjen G (2007) Seizure-like after discharges simulated in a model neuron. *J Comput Neurosci* 22(2):105–128 (24)
- Larsen BR, Assentoft M, Cotrina ML et al (2014) Contributions of the  $\text{Na}^+/\text{K}^+$ -ATPase, NKCC1, and Kir4.1 to hippocampal  $\text{K}^+$  Clearance and volume responses. *Glia* 62(4):608–622
- Marom M et al (2003) Depolarization block of neurons during maintenance of electrographic seizures. *J Neurophysiol* 90(4):2402–2408
- Moujahid A, D'Anjou A, Torrealdea FJ et al (2012) Energy and information in Hodgkin–Huxley neurons. *Phys Rev E* 83(3):681–689
- Ohno Y, Tokudome K, Kunisawa N et al (2015) Role of astroglial Kir4.1 channels in the pathogenesis and treatment of epilepsy. *Ther Targets Neurol Dis* 2:1–10
- Østby I, Øyehaug L, Einevoll GT, Nagelhus EA, Plahte E, Zeuthen T, Lloyd CM, Ottersen OP, Omholt SW (2009) Astrocytic mechanisms explaining neural-activity-induced shrinkage of extraneuronal space. *PLoS Comput Biol* 5(1):291–298
- Øyehaug L, Østby I, Lloyd CM et al (2012) Dependence of spontaneous neuronal firing and depolarisation block on astroglial membrane transport mechanisms. *J Comput Neurosci* 32(1):147–165
- Park EH, Durand DM (2006) Role of potassium lateral diffusion in non-synaptic epilepsy: a computational study. *J Theor Biol* 238(3):666–682
- Pinsky PF, Rinzel J, Pinsky PF et al (1994) Intrinsic and network rhythmogenesis in a reduced Traub model for CA3 hippocampal neurons. *J Comput Neurosci* 1(1–2):39–60
- Prinz AA (2008) Understanding epilepsy through network modeling. *Proc Natl Acad Sci USA* 105(16):5953–5954
- Traynelis SF, Dingledine R (1988a) Potassium-induced spontaneous electrographic seizures in the rat hippocampal slice. *J Neurophysiol* 59(1):259–276
- Ullah G, Schiff SJ (2010) Assimilating seizure dynamics. *PLoS Comput Biol* 6(5):e1000776–e1000776
- Ullah G, Cressman JR Jr, Barreto E et al (2009) The influence of sodium and potassium dynamics on excitability, seizures, and the stability of persistent states: II. Network and glial dynamics. *J Comput Neurosci* 26(2):171–183
- Wendling F, Bartolomei F, Mina F et al (2012) Interictal spikes, fast ripples and seizures in partial epilepsies—combining multi-level computational models with experimental data. *Eur J Neurosci* 36(2):2164–2177
- Yaari Y, Konnerth A, Heinemann U (1986) Nonsynaptic epileptogenesis in the mammalian hippocampus in vitro. II. Role of extracellular potassium. *J Neurophysiol* 56(2):424–438
- Yina W, Ghanim U, Justin I et al (2014a) Oxygen and seizure dynamics: II. Computational modeling. *J Neurophysiol* 112(2):213–223
- Yina W, Ghanim U, Schiff SJ (2014b) Unification of neuronal spikes, seizures, and spreading depression. *J Neurosci* 34(35):11733–11743
- Ziburkus J et al (2006) Interneuron and pyramidal cell interplay during in vitro seizure-like events. *J Neurophysiol* 95(6):3948–3954
- Žiburkus J, Cressman JR, Schiff SJ (2013) Seizures as imbalanced up states: excitatory and inhibitory conductances during seizure-like events. *J Neurophysiol* 109(5):1296–1306